Middle East Journal of Applied Sciences
Volume: 15 | Issue: 04| Oct. – Dec. | 2025

EISSN: 2706 -7947 ISSN: 2077- 4613
DOI: 10.36632/mejas/2025.15.4.19
Journal homepage: www.curresweb.com
Pages: 232-251

Evaluation of Nanomaterials (Copper, Silver, and Chitosan) in management of Downy Mildew Disease on Basil (*Ocimum basilicum*)

Eslam M. Abdullah[1], Raouf N. Fawzy[2], Khaled S. Eid[2], Gamal A. Ahmed[2], Ahlam M. Gwaily[1] and Agha M. K. M. [1]

[1]Plant Protection Department, Ecology and Drylands Division, Desert Research Center (DRC), Cairo, Egypt.
[2]Plant Pathology Department, Faculty of Agriculture, Benha University, Mushtuhur, Qalyubia, Egypt.

Received: 24 July 2025 **Accepted:** 30 Sept. 2025 **Published:** 20 Oct. 2025

ABSTRACT

Basil downy mildew (BDM), caused by the oomycete *Peronospora belbahrii*, is a devastating foliar disease that causes severe yield losses in basil production. This study evaluated the antifungal potential of biosynthesized copper (Cu), chitosan (Cs), and silver (Ag) nanoparticles as eco-friendly alternatives to synthetic fungicides. The efficacy of these nanomaterials (50–400 mg L^{-1}) was evaluated against potassium silicate and the fungicide Redomil Gold in laboratory and greenhouse trials. *In vitro* assays showed CuNPs (400 mg L^{-1}) had the highest inhibition of conidial germination (96.7%), performing slightly better than Redomil Gold (96.4%) and CNPs (96.0%). In preventive greenhouse trials, CNPs (400 mg L^{-1}) provided protection statistically comparable to Redomil Gold. The most significant finding was in the curative trial, where CuNPs (400 mg L^{-1}) demonstrated significantly *superior* efficacy to the fungicide, reducing final disease severity to 16.0% (compared to 27.6% for Redomil Gold). Furthermore, CuNPs and CNPs acted as biostimulants, significantly improving plant anatomical structure, growth parameters, and the induction of defense-related enzymes (e.g., PO, PPO, CAT) and phenols. These results demonstrate that biosynthesized nanoparticles, particularly CuNPs, offer a highly effective, dual-action approach for controlling BDM, acting as both a direct antifungal and a plant defense elicitor.

Keywords: Basil, downy mildew, *Peronospora belbahrii,* antifungal, nanoparticles, eco-friendly

1. Introduction

Basil (*Ocimum spp.*) is one of the most important aromatic plants in terms of economic value and productivity, representing a significant source of income for large-scale herb producers around the world, where it is grown in fields, high tunnels, and greenhouses (Simon *et al*., 1999). Basil downy mildew (BDM), caused by *Peronospora belbahrii*, has become a major problem in sweet basil (*O. basilicum*) cultivation across the world in the last decade. Since its emergence in 2007, it has caused tens of millions of dollars in losses in the United States alone and has been described as a damaging disease in several countries (Wyenandt *et al*., 2015; Abdullah et al., 2022).

In Egypt, since the oomycete pathogen (*P. belbahrii*) was initially discovered, mainly in the Beni-Suef governorate in 2013, it has spread swiftly and become a pandemic disease in all basil-growing regions. It is considered the source of severe disease and total crop losses, as infected basil plants are no longer marketable (Ghebrial & Nada, 2017).

Fungicides, as a conventional method to control plant pathogens, have affected both the environment and the economy of farmers. As much as 90% of applied fungicides can be lost in the open field during application and as overland flow, affecting both agriculture and the environment, while also increasing application costs for the farmer. Thus, the environmental problems caused by fungicide overuse have been a matter of concern for both scientists and the public. The reasons for this are dual:

Corresponding Author: Eslam M. Abdullah, Plant Protection Department, Ecology and Drylands Division, Desert Research Center (DRC), Cairo, Egypt.

(1) the high toxicity and non-biodegradable properties of pesticides and (2) the excessive pesticide residues in soil, water resources, and crops that influence human and animal health (Koul *et al*., 2008). The use of nanotechnology as an alternative to develop eco-safe antifungal agents, like bio-based nanomaterials, is urgently needed to fight against fungal pathogens and replace conventional, high-toxicity pesticides. The expression "nano-fungicides" is used to describe any fungicide formulation that: (a) intentionally includes entities in the nanometer size range (up to 100 nm) and (b) is claimed to have novel properties associated with this small size (Abd-Elsalam and Alghuthaymi, 2015).

The importance of using nanotechnology is due to the ability of nanoparticles to improve the stability of the active compound against environmental degradation, such as oxidation, hydrolysis, and enzymatic decomposition. The particle size and distribution of nanoparticles are their most important characteristics, as they can determine their distribution, toxicity, and delivery ability to the target (Kim *et al*., 2009; Li *et al*., 2011).

Synthesis of nanoparticles using biological entities has attracted great interest due to their unusual optical properties (Krolikowska *et al*., 2003). Bio-nanotechnology has emerged as an integration between biotechnology and nanotechnology for developing biosynthesis and environmentally friendly technology for the synthesis of nanomaterials. The synthesis and assembly of nanoparticles would benefit from the development of clean, non-toxic, and environmentally acceptable "green chemistry" procedures (Bhattacharya & Rajinder, 2005).

Concurrently, potassium silicate has been recognized as a promising eco-friendly alternative, primarily by enhancing plant resistance. It is reported to strengthen plant cell walls and induce systemic resistance by triggering defense-related enzymes, thereby reducing disease severity and enhancing overall plant vigor (Ghebrial & Nada, 2017).

Although nanomaterials like copper, silver, and chitosan have demonstrated broad-spectrum antifungal properties against various plant pathogens (Okey-Onyesolu *et al*., 2021), their specific efficacy against *Peronospora belbahrii* remains largely unexplored. Furthermore, comprehensive reviews on BDM management focus primarily on fungicides and genetic resistance, highlighting a gap in the literature regarding nano-based interventions (Wyenandt *et al*., 2015). This highlights the need to evaluate and compare these eco-friendly alternatives against conventional fungicides.

This study aims to evaluate the effectiveness of biosynthesized copper, chitosan, and silver nanoparticles, along with potassium silicate and the fungicide Redomil Gold, in inhibiting spore germination and reducing the incidence and severity of basil downy mildew. The evaluation includes a comprehensive assessment of their antifungal properties, potential disease suppression mechanisms, and overall impact on plant health. The study also aims to compare the efficacy of these treatments in mitigating disease progression and enhancing plant resistance. It is hypothesized that the biosynthesized nanoparticles, particularly silver, will provide disease control comparable to the synthetic fungicide (Redomil Gold) but with significantly enhanced plant health indicators, while potassium silicate will primarily act by inducing systemic resistance.

2. Materials and Methods

2.1. Preparation of nanomaterials

2.1.1. Chitosan nanoparticles (CNPs) chemicals and reagents: Chitosan (85% deacetylation) was procured from (STARCHEMIC), sodium tripolyphosphate (STPP) from (SRL company), and glacial acetic acid were used without further purification.

Preparation of Chitosan Nanoparticles: Chitosan nanoparticles were prepared based on the ionic gelation method reported by Tang *et al*. (2007) using STPP as an anionic cross-linker. Briefly, 0.2 g of chitosan was dissolved in 61.3 mL of a 1% (v/v) aqueous acetic acid solution. The STPP solution was prepared by dissolving 0.069 g of STPP in 6.6 mL of distilled water. The STPP solution was then added dropwise to the chitosan solution under magnetic stirring (1000 rpm, 1 hour) at room temperature.

2.1.2. Copper Nanoparticles (CuNPs) Culturing of *Pseudomonas fluorescens*: *P. fluorescens* (obtained from the Department of Plant Pathology, DRC culture collection) was grown in King's B (KB) medium. The inoculum was transferred to KB broth and incubated at 30°C in a shaking incubator at 150 rpm.

Biosynthesis of CuNPs by P. fluorescens: Copper nanoparticles were synthesized using *P. fluorescens* as described by Shantkriti and Rani (2014). After 48 h of growth, the culture was centrifuged at 7500

rpm for 20 min at 30°C. The cell-free culture supernatant was recovered and centrifuged again at 10,000 rpm for 20 min at 30°C. For the synthesis, 100 mL of the cell-free supernatant was mixed with 100 mL of a 1 mM $CuSO_4$ solution and placed in a shaking incubator for 24 to 48h at 30°C, 150 rpm.

2.1.3. Silver nanoparticles (AgNPs): Silver nanoparticles were prepared according to Abu-Elsaoud *et al*. (2015) using the fungus *Trichoderma viride* (obtained from the Department of Plant Pathology, DRC culture collection).

Biomass preparation: *T. viride* was grown on potato dextrose agar (PDA) slants at 25°C for 14 days. The cultures were then grown in 250-mL Erlenmeyer flasks containing 100 mL potato dextrose broth (PDB) at 25°C and 120 rpm for 5 days. The biomass was harvested by filtration through sterile Whatman No. 1 filter paper. The filtrate (fungal crude extract) was collected and used for nanoparticle synthesis.

Biosynthesis of AgNPs: For biosynthesis, 50 mL of the cell filtrate was mixed with an aqueous $AgNO_3$ solution to achieve a final concentration of 1 mM. A reaction mixture without $AgNO_3$ was used as a control. The solutions were incubated at 28°C for 24h in the dark to avoid photochemical reactions. The AgNPs were purified by centrifugation at 10,000 rpm for 10 min (repeated twice) and collected for further characterization.

2.2. Characterization of nanoparticles

The preliminary detection of synthesis was carried out by visual observation of color change.
UV–visible spectrophotometer (UV–vis): The samples were subjected to optical measurements using a UV-Vis spectrophotometer (LW-200 Series). Spectra were scanned between 200 and 800 nm at a resolution of 1 nm.

Particle size distribution (DLS): The particle size distribution of the nanocomposite samples dispersed in DI water was examined by DLS (Dynamic light scattering) (NICOMP N3000, particle size analyzer).

Transmission Electron Microscopy (TEM): The particle size and morphology of the silver nanoparticles were analyzed using Transmission Electron Microscope (TEM).

2.3. Effect of nanomaterials and potassium silicate on conidia germination *(In vitro*)

This experiment evaluated the effect of nanomaterials and potassium silicate compared with Redomil Gold fungicide on *P. belbahrii* conidial germination. The water suspension of conidia was mixed with the treatments. The final concentrations tested were: chitosan NPs, copper NPs, and silver NPs (50, 100, 200, and 400 mg L^{-1}); and potassium silicate (1.0, 1.5, 2.0, and 3.0 g L^{-1}). Redomil Gold was used as the recommended dosage (Kasprowicz *et al*., 2010).

Infected basil leaves were brought to the laboratory. Conidia were harvested with the help of a small sterile paintbrush into a Petri plate containing sterile distilled water. A 20 µL drop of the spore suspension was placed onto a cavity slide. Three replications were made for each treatment, and the slides were incubated for 24 h at 18°C in 95% RH. The germination percentage was calculated under a light microscope.

2.4. Control of BDM under greenhouse conditions

Seeds were planted in a growth chamber, and seedlings were transplanted into pots (4 seedlings/pot). Three replicates were used for each treatment. Two protocols were evaluated:

2.4.1. Preventive (Prophylactic) Treatment The experiment was conducted with four concentrations of each material: NPs (50, 100, 200, and 400 mg L^{-1}) and potassium silicate (1.0, 1.5, 2.0, and 3.0 g L^{-1}). The fungicide (Redomil Gold MZ 68 WG) was used at the recommended dosage. Materials were sprayed on plants 3 days prior to inoculation with *P. belbahrii*. Three replicates for each concentration and 3 non-treated replicates (control) were used. This experiment was conducted on the first of June in the Nanophytopathology lab greenhouse, DRC, Cairo, Egypt. Artificial inoculation was performed at the four-true-leaf stage. Data for disease incidence and severity were recorded weekly for one month.

2.4.2. Treatment Plants were first artificially inoculated at the four-true-leaf stage. The same materials and concentrations were applied to the plants immediately after the first symptoms of infection appeared. Data on disease incidence and severity were recorded weekly for one month and compared to the infected control.

2.5. Measurements

2.5.1. Leaf anatomy:

Leaf Anatomy of basil plants a comparative microscopical examination was performed on plant material (main stem and corresponding leaf lamina) from the control and the treatments showing the most positive response. Specimens were taken 45 days after sowing (one week after the last treatment application). Specimens were killed and fixed for at least 48 h in F.A.A. (10 mL formalin, 5 mL glacial acetic acid, 85 mL 70% ethyl alcohol). Samples were washed, dehydrated in a normal butyl alcohol series, embedded in paraffin wax (56°C m.p.), sectioned to a 20 µm thickness, double-stained with crystal violet-erythrosine, cleared in xylene, and mounted in Canada balsam (Nassar and El-Sahhar, 1998).

2.5.2. Biochemical analysis

Determination of total phenolic compounds: The total phenolic content of 70% methanolic extracts was determined by the Folin–Ciocalteu method (Kaur and Kapoor, 2002). Absorbance was measured at 650 nm. Results were expressed as mg of gallic acid equivalent per g dry weight (mg GAE g^{-1} DW).

Determination of total protein: Total nitrogen content was determined using the Micro-Kjeldahl method according to the British Pharmacopoeia (1993).

Determination of total carbohydrates: Hydrolysable carbohydrates were extracted by digesting 1 g of plant powder with 2.5 mL of 2 M HCl at 100°C for 90 min. Sugars were estimated using the phenol-sulfuric acid assay. Absorbency was measured at 490 nm. The concentration of total sugars (g %) was determined **(Chaplin and Kennedy, 1994).**

Determination of total Lipids: One hundred grams of air-dried plant powder was extracted with petroleum ether (40-60°C): diethyl ether (1:1) for 24 hours using a Soxhlet apparatus. The lipids were obtained by distilling off the solvent and heating them in a vacuum oven at 50°C to a constant weight **(Christie, 1982).**

2.5.3. Enzyme activities

Peroxidase (PO): PO activity was determined based on the oxidation of pyrogallol according to Allam and Hollis (1972). Peroxidase activity was expressed as the change in absorbance at 425 nm min^{-1} g^{-1} fresh weight (FW).

Polyphenol oxidase (PPO): PPO activity was measured using catechol as a substrate as described by Matta and Dimond (1963). PPO activity was expressed as the change in absorbance at 420 nm min^{-1} g^{-1} FW.

Catalase (CAT): CAT activity was measured spectrophotometrically using the ammonium molybdate method **(Goth, 1991).** One unit (U) of CAT is the amount of enzyme that decomposes 1 µM of H_2O_2 per minute. CAT activity was expressed as U mg^{-1} protein.

2.5.4. Essential oil content

Isolation of essential oils: Air-dried basil samples (10 g) were hydro-distilled in a Clevenger apparatus **(Guenther, 1961).** The essential oil percentage (%) was determined. The oils were collected, dehydrated over anhydrous sodium sulfate, and stored in a refrigerator.

Gas chromatography (GC) analysis of essential oils: GC analysis was performed on a Ds Chrom 6200 Gas Chromatograph with a Flame Ionization Detector (FID). Column: BPX-5 (30 m length, 0.25 mm diameter). A 1 µL sample size was injected. The temperature ramped from 70°C to 200°C at

10°C/min. Detector (FID) temperature was 280°C. Carrier gas was Nitrogen (N_2). Flow rates were 30 mL/min for N_2, 30 mL/min for H_2, and 300 mL/min for air. Compounds were identified by comparing their retention times to those of authentic standards. The relative percentage of each component was calculated from the peak area (Ghebrial and Dewidar, 2020). Extractions were carried out at the Medicinal and Aromatic Plants Research Dept. (DRC), and GC analysis was carried out at the DRC central laboratory.

Statistical analysis:

The obtained results were exposed to statistical analysis of either simple regression & correlation or analysis of variance (ANOVA) according to the eligibility of the data set. Generally, whenever there is enough replication, the ANOVA will be recruited according to the randomized complete blocks statistical design according to the procedures described by Gomez and Gomez (1984). SPSS package was recruited to carry out both methodologies adopted for statistical analysis in the current research work. The differences between the mean values of various treatments were compared by Duncan's multiple range test **(Duncan, 1955)**.

3. Results

3.1. Preparation and characterization of nanoparticles

3.1.1. Chitosan nanoparticles (CNPs)

The successful synthesis of chitosan nanoparticles (CNPs) was confirmed through UV-Vis, DLS, and TEM analyses.

UV-Vis Spectrophotometry: The UV-Vis spectrum of the synthesized CNPs (Fig. 1) showed a strong and broad absorption peak in the range of 450–510 nm, confirming the formation of the nanoparticles.

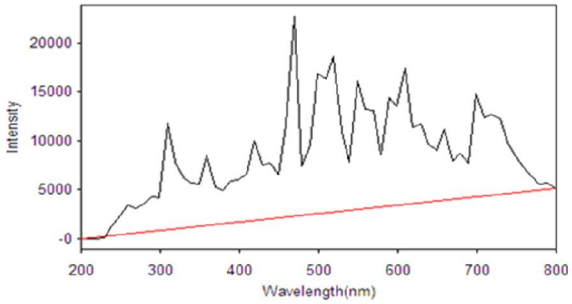

Fig. 1: UV-Vis spectrum shows absorption peak of synthesized chitosan NPs.

Particle size distribution (DLS): Dynamic Light Scattering (DLS) analysis was used to determine the hydrodynamic size distribution. The results (Fig. 2) showed that the CNPs had an average hydrodynamic diameter of 34.1 nm.

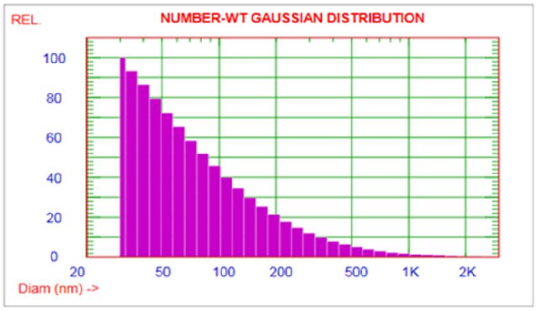

Fig. 2: DLS spectra of the chitosan nanoparticles

Transmission electron microscopy (TEM): TEM analysis revealed the morphology and core size of the CNPs (Fig. 3). The nanoparticles were observed to be uniform, spherical, and had an average particle size ranging from 4.9 to 12.7 nm.

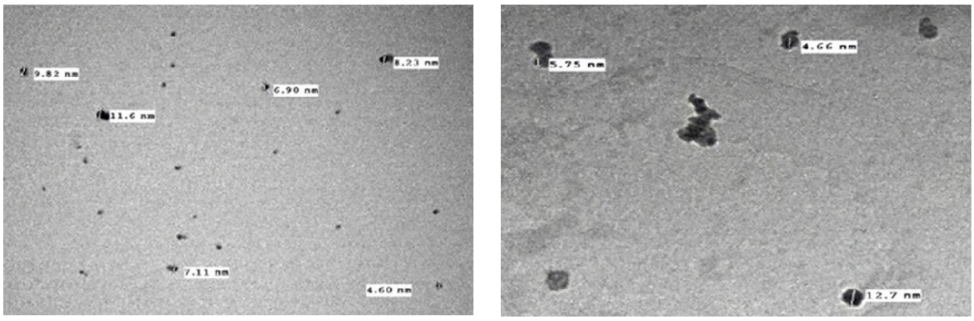

Fig. 3: Transmission electron microscope (TEM) image of chitosan nanoparticles

3.1.2. Copper nanoparticles (CuNPs)

Visual observation: Biosynthesis of CuNPs was first indicated by a visual color change. Upon incubation of the *P. fluorescens* cell-free supernatant with the $CuSO_4$ solution for 48 hours, the color of the reaction mixture shifted from blue to dark green, suggesting the formation of CuNPs.

UV–visible spectrophotometry (UV–vis): The UV-Vis absorption spectrum (Fig. 4) confirmed this formation, showing a broad absorption band with characteristic peaks observed between 490 nm and 700 nm.

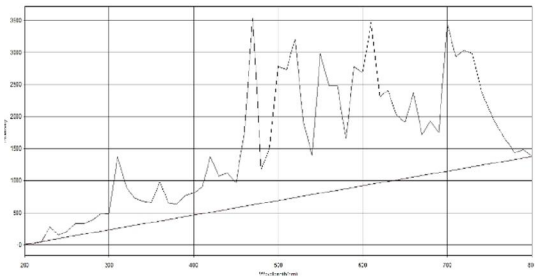

Fig. 4: UV-Vis spectrum shows absorption peak of synthesized CuNPs.

Particle size distribution (DLS): DLS analysis (Fig. 5) determined the average hydrodynamic diameter of the biosynthesized CuNPs to be 49.4 nm.

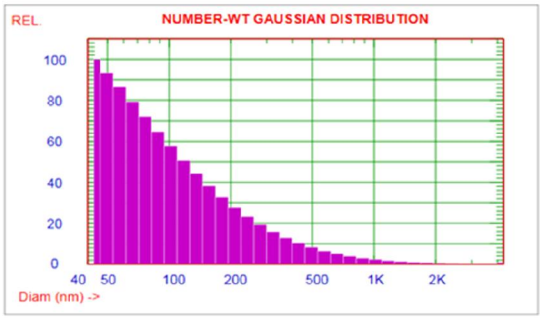

Fig. 5: DLS spectra of the copper Cu-NPs

Transmission electron microscopy (TEM): TEM analysis was used to determine the morphology and size of the CuNPs (Fig. 6). The images showed nanoparticles with both spherical and hexagonal shapes, possessing a particle size ranging from 37.4 to 59.1 nm.

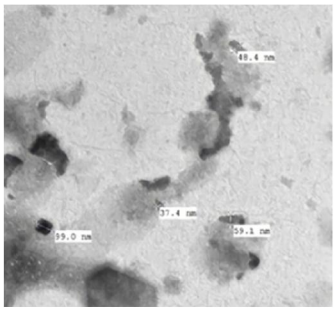

Fig. 6: Transmission electron microscope (TEM) image of Cu-NPs

3.1.3. Silver Nanoparticles (AgNPs)

Visual observation: Preliminary confirmation of AgNPs biosynthesis was obtained through visual observation. The *T. viride* fungal filtrate, upon addition of the $AgNO_3$ solution, changed color from its original yellowish-brown to a dark brown, indicating AgNPs formation.

UV–visible spectrophotometry (UV–vis): The UV-Vis spectrum (Fig. 7) showed a strong, wide absorption peak with a maximum (λ_max_) centered between 480 nm and 710 nm. This characteristic peak is attributed to the Surface Plasmon Resonance (SPR) of the synthesized AgNPs.

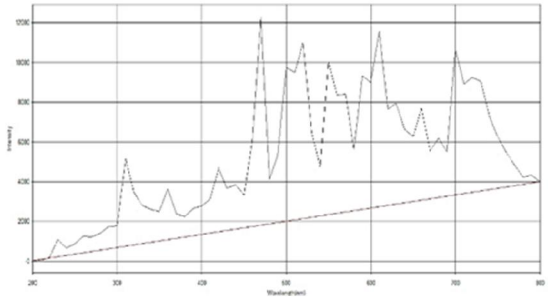

Fig 7: UV-Vis spectrum shows absorption peak of synthesized AgNPs.

Particle size distribution (DLS): The DLS measurement (Fig. 8) indicated that the AgNPs had an average hydrodynamic diameter of 32.8 nm.

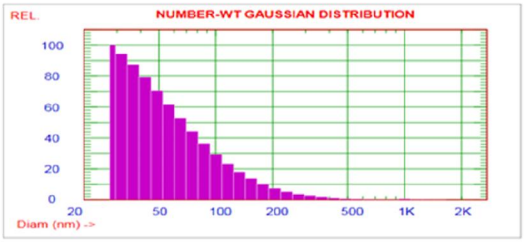

Fig 8: DLS spectra of the Ag-NPs

Transmission electron microscopy (TEM): TEM analysis (Fig. 9) confirmed the size and morphology of the nanoparticles. The AgNPs were observed to be spherical in shape, with an average particle size ranging from 19.3 to 23.5 nm.

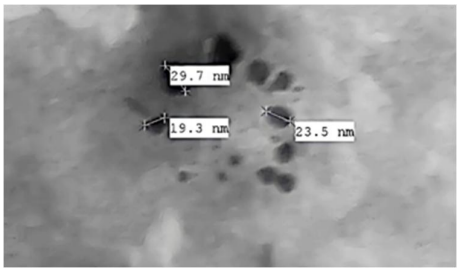

Fig. 9: Transmission electron microscope (TEM) image of Ag-NPs

3.2. Effect of nanomaterials and potassium silicate on conidial germination (*In vitro*)

All tested nanomaterials, potassium silicate, and the fungicide Redomil Gold caused a significant decrease in *P. belbahrii* conidial germination compared to an untreated control (Table 1 and Fig. 10). A clear dose-dependent relationship was observed for all treatments, where higher concentrations resulted in higher inhibition percentages. At the highest tested concentration (400 mg L^{-1}), Copper NPs (CuNPs) showed the highest efficacy, inhibiting 96.7% of conidial germination. This was slightly higher than the commercial fungicide Redomil Gold (96.4%) and Chitosan NPs (96.0%). Silver NPs at the same concentration also showed strong inhibition (93.4%). Potassium silicate showed the lowest (though still significant) inhibitory effect across its tested concentrations, achieving 83.0% inhibition at 3 mL. Overall, CuNPs had the lowest mean germination (5.83%), followed by Chitosan NPs (7.50%).

Table 1: Effect of (chitosan- copper- silver) Nanoparticles, potassium silicate in different concentrations, and Redomil gold in recommended dosage on germination and inhibition percentage of *P. belbahrii* conidia.

Treatment	Con.	Germination %	Inhibition %
Chitosan NPs	**50 mg L^{-1}**	10.0	90.0
	100 mg L^{-1}	9.0	91.0
	200 mg L^{-1}	7.0	93.0
	400 mg L^{-1}	4.0	96.0
Mean		7.50	92.50
Copper NPs	**50 mg L^{-1}**	8.3	91.7
	100 mg L^{-1}	6.3	93.7
	200 mg L^{-1}	5.3	94.7
	400 mg L^{-1}	3.3	96.7
Mean		5.83	94.17
Silver NPs	**50 mg L-^{1}**	12.6	87.4
	100 mg L^{-1}	11.3	88.7
	200 mg L^{-1}	10.3	89.7
	400 mg L^{-1}	6.6	93.4
Mean		10.25	89.75
Potassium Silicate	**1 mL**	26	74.0
	1.5 mL	23.3	76.7
	2 mL	20	80.0
	3 mL	17	83.0
Mean		21.58	78.42
Redomil Gold MZ 68 WG		3.6	96.4
LSD 1 %		**Treatments**	**1.46**
		Concentrations	**1.31**
		Interaction	**2.92**

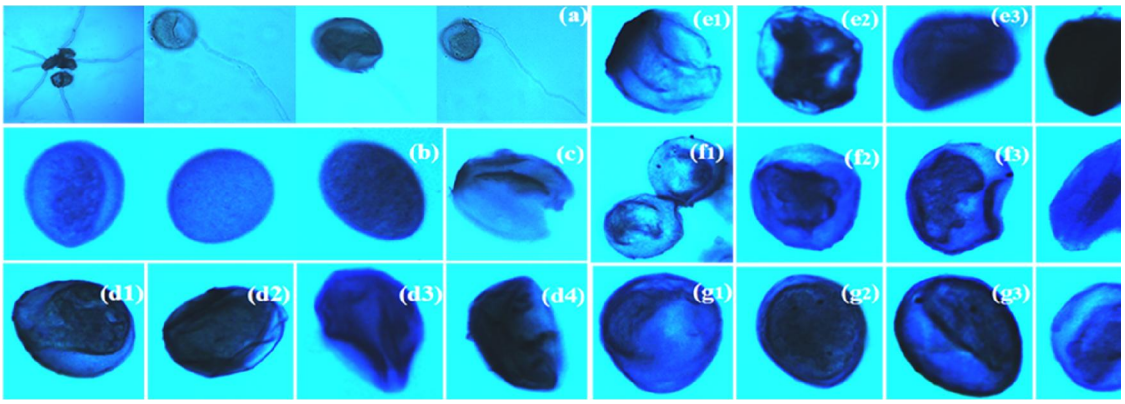

Fig. 10: Effect of different Nano-particles and potassium silicate with various concentration; (a) conidial germination, (b) control, (c) Redomil Gold MZ, (d 1,2,3,4) Copper NPs 50, 100, 200, 400 mg L^{-1}; (e 1,2,3,4) Silver NPs 50, 100, 200, 400 mg L^{-1}; (f 1,2,3,4) Chitosan NPs 50, 100, 200, 400 mg L^{-1}; (g 1,2,3,4) potassium silicate 1 mL, 1.5 mL, 2mL, 3mL. * Under light microscope 40X microscope lens.

3.3. Greenhouse Experiment 1: Preventive (Prophylactic) Application

In the preventive trial, treatments were applied 3 days *before* artificial inoculation. All treatments significantly reduced the Disease Incidence (DI) and Disease Severity (DS) over four weeks compared to the untreated control (Table 2). After four weeks of observation, the most effective treatment was the commercial fungicide Redomil Gold (DI: 36.0%, DS: 34.3%). Chitosan NPs at 400 mg L^{-1} provided statistically comparable protection (DI: 36.7%, DS: 34.7%), showing no significant difference from the fungicide. Potassium silicate (3 mL) also performed well (DI: 40.0%, DS: 38.0%), followed by the highest concentration of CuNPs (DI: 46.6%, DS: 40.5%). Silver NPs showed the least protective effect in this trial, with the 50 mg L^{-1} concentration being the least effective of all treatments (DI: 64.3%, DS: 56.0%). All treatments performed significantly better than the untreated control (DI: 100%, DS: 98.7%). In the curative trial, treatments were applied *after* the first symptoms of infection appeared (Table 3). This trial yielded the most significant finding of the study. After four weeks, Copper NPs at 400 mg L^{-1} emerged as the most effective treatment overall. It significantly suppressed the disease, showing the lowest final Disease Incidence (27.0%) and Disease Severity (16.0%). This was followed by Chitosan NPs at 400 mg L^{-1} (DI: 41.7%, DS: 21.0%). Notably, both the 400 mg L^{-1} CuNPs and CNP treatments demonstrated significantly better disease control than the commercial fungicide Redomil Gold (DI: 49.3%, DS: 27.6%). Silver NPs and Potassium silicate were the least effective treatments in this curative trial. Potassium silicate at 1 mL showed the highest disease levels (DI: 67.7%, DS: 52.3%), though all treatments were still statistically superior to the untreated control (DI: 100%, DS: 96.3%).

Table 2: Effect of (chitosan-copper-silver) Nanoparticles, potassium silicate in different concentrations, and Redomil gold MZ 68 WG in recommended dosage under greenhouse conditions showing disease incidence % and disease severity % before artificial infection.

(a) Effect of treatment x infection progress

Treatment		Week 1		Week 2		Week 3		Week 4	
		DI %	DS%	DI %	DS%	DI %	DS%	DI %	DS%
Chitosan NPs	50 mg L^{-1}	32.0	26.0	40.7	35.0	46.3	40.6	50.0	46.3
	100 mg L^{-1}	27.0	21.7	37.0	31.6	43.0	36.0	47.0	43.0
	200 mg L^{-1}	22.5	18.0	30.7	27.5	38.7	31.0	42.0	40.0
	400 mg L^{-1}	19.0	15.0	27.5	20.6	33.0	24.0	36.7	34.7
Copper NPs	50 mg L^{-1}	43.0	39.0	49.5	45.3	54.0	48.5	60.0	56.0
	100 mg L^{-1}	38.5	36.0	44.3	41.3	50.3	44.6	56.5	51.0
	200 mg L^{-1}	32.6	31.0	39.6	37.0	45.0	39.0	49.5	45.3
	400 mg L^{-1}	29.7	28.5	38.3	31.7	41.0	36.0	46.6	40.5
Silver NPs	50 mg L^{-1}	47.3	41.6	55.5	49.6	61.3	49.7	64.3	56.0
	100 mg L^{-1}	41.0	37.6	47.0	42.0	51.3	47.0	61.3	51.6
	200 mg L^{-1}	37.0	34.0	41.0	38.0	49.7	41.3	57.3	49.0
	400 mg L^{-1}	31.3	32.5	36.5	34.7	45.3	37.7	52.0	42.0
Potassium Silicate	1 mL	31.6	30.3	43.0	39.3	48.3	40.3	53.5	49.3
	1.5 mL	28.7	27.6	38.0	31.0	43.4	35.3	48.5	44.3
	2 mL	23.5	21.6	34 .0	29.0	40.3	32.0	44.0	42.6
	3 mL	21.0	19.6	30.0	23.0	35.7	28.0	40.0	38.0
Redomil Gold MZ 68 WG		18.6	17.3	23.0	20.3	29.0	27.0	36.0	34.3
Control		95.0	92.7	96.3	96.0	100	97.3	100	98.7

* Disease incidence (DI), Disease severity (DS)

(b) Effect of treatment x concentration interaction

Treatment		Disease incidence %	Disease severity%
Chitosan NPs	50 mg L^{-1}	42.3	37.0
	100 mg L^{-1}	38.5	33.1
	200 mg L^{-1}	33.5	29.2
	400 mg L^{-1}	29.1	23.6
Mean		30.7	35.8
Copper NPs	50 mg L^{-1}	51.7	47.3
	100 mg L^{-1}	47.5	43.3
	200 mg L^{-1}	41.8	39.0
	400 mg L^{-1}	38.8	34.3
Mean		40.9	44.9
Silver NPs	50 mg L^{-1}	57.2	49.3
	100 mg L^{-1}	50.2	44.6
	200 mg L^{-1}	46.3	40.6
	400 mg L^{-1}	41.3	36.8
Mean		42.8	48.7
Potassium Silicate	1 mL	44.2	39.8
	1.5 mL	39.7	34.6
	2 mL	35.5	31.2
	3 mL	31.7	27.3
Mean		33.2	37.8
Redomil Gold MZ 68 WG		24.8	26.7
Control		96.2	97.8
LSD 1 %	Treatments	1.00	1.14
	Concentrations	0.81	0.93
	TxC	2.0	2.3

(c) Effect of treatment x Weeks interaction

Treatment		1st week	2nd week	3rd week	4th week	Mean
Disease incidence %	Chitosan NPs	25.2	34.0	40.3	43.9	35.8
	Copper NPs	36.0	43.0	47.6	53.1	44.9
	Silver NPs	39.2	45.1	51.9	58.8	48.7
	Potassium Silicate	26.3	36.3	41.9	46.6	37.8
	Redomil gold	18.7	23.0	29.0	36.0	26.7
	Control	95.0	96.3	100.0	100.0	97.8
	Weeks Mean	40.0	46.3	51.8	56.4	48.6
	LSD 1 %		Weeks		WxT	
			0.81		2.0	
Disease severity %	Chitosan NPs	20.2	28.8	32.9	41.0	30.7
	Copper NPs	33.8	39.7	42.1	48.3	40.9
	Silver NPs	36.5	41.1	43.9	49.7	42.8
	Potassium Silicate	24.7	30.8	33.9	43.6	33.2
	Redomil gold	17.3	20.3	27.0	34.3	24.8
	Control	92.7	96.0	97.3	98.7	96.2
	Weeks Mean	37.5	42.8	46.2	52.6	44.8
	LSD 1 %		Weeks		WxT	
			0.93		2.3	

Table 3: Effect of (Chitosan- Copper- Silver) Nanoparticles, potassium silicate in different concentrations, and Redomil gold in recommended dosage under greenhouse conditions showing Disease incidence % and Disease severity % after artificial infection.

(a) Effect of treatment x infection progress

Treatment	Con.	Week 1		Week 2		Week 3		Week 4	
		DI %	DS %	DI %	DS %	DI %	DS %	DI %	DS %
Chitosan NPs	50 mg L-1	100	87.0	98.0	84.0	63.0	38.3	51.3	35.0
	100 mg L-1	100	85.3	95.0	81.3	58.0	36.0	47.0	30.0
	200 mg L-1	99.0	81.5	92.0	77.5	52.7	33.3	44.0	26.7
	400 mg L-1	98.6	80.3	90.3	73.0	47.0	26.4	41.7	21.0
Copper NPs	50 mg L-1	100	86.0	95.0	81.0	62.0	38.0	45.6	26.0
	100 mg L-1	100	83.0	93.3	79.0	56.0	32.5	35.0	23.0
	200 mg L-1	98.0	81.3	90.3	75.5	51.3	30.0	32.6	21.5
	400 mg L-1	96.3	79.0	89.0	71.0	35.0	25.0	27.0	16.0
Silver NPs	50 mg L-1	100	89.0	98.0	84.7	83.0	55.7	56.3	48.5
	100 mg L-1	100	86.0	97.0	81.3	78.7	51.6	52.5	41.6
	200 mg L-1	98.3	84.3	96.0	78.3	75.0	47.7	48.6	40.0
	400 mg L-1	98.0	79.5	95.0	72.0	70.7	44.3	37.0	38.6
Potassium Silicate	1 mL	100	90.0	99.0	86.0	87.0	57.6	67.7	52.3
	1.5 mL	100	88.0	98.3	81.7	81.0	54.0	64.0	47.0
	2 mL	100	85.0	97.0	78.6	77.0	49.0	60.0	41.6
	3 mL	99.0	82.0	96.5	77.3	71.5	45.0	58.0	38.0
Redomil Gold MZ 68 WG		77.0	78.7	65.0	75.5	57.5	39.6	49.3	27.6
Control		100	92.0	100	93.0	100	95.0	100	96.3

* Disease incidence (DI), Disease severity (DS)

(b) Effect of treatment x concentration interaction

Treatment	Con.	Disease incidence %	Disease severity %
Chitosan NPs	**50 mg L^{-1}**	78.1	61.1
	100 mg L^{-1}	75.0	58.2
	200 mg L^{-1}	71.9	54.8
	400 mg L^{-1}	69.4	50.2
Mean		56.1	73.6
Copper NPs	**50 mg L^{-1}**	75.7	57.8
	100 mg L^{-1}	71.1	54.4
	200 mg L^{-1}	68.1	52.2
	400 mg L^{-1}	61.8	47.8
Mean		53.0	69.2
Silver NPs	**50 mg L^{-1}**	84.3	69.5
	100 mg L^{-1}	82.1	65.2
	200 mg L^{-1}	79.5	62.6
	400 mg L^{-1}	75.2	58.7
Mean		64.0	80.3
Potassium Silicate	**1 mL**	88.4	71.5
	1.5 mL	85.8	67.7
	2 mL	83.5	63.6
	3 mL	81.3	60.6
Mean		65.8	84.8
Redomil Gold MZ 68 WG		55.4	62.3
Control		94.1	100.0
LSD 1 %	**Treatments**	0.76	1.03
	Concentrations	0.62	0.84
	TxC	1.52	2.05

(c) Effect of treatment x weeks interaction

	Treatment	1st week	2nd week	3rd week	4th week	Mean
Disease incidence %	**Chitosan NPs**	99.4	93.8	55.2	46.0	73.6
	Copper NPs	98.6	91.9	51.1	35.1	69.2
	Silver NPs	99.1	96.5	76.8	48.7	80.3
	Potassium Silicate	99.8	97.8	79.2	62.4	84.8
	Redomil gold	77.0	65.0	57.7	49.3	62.3
	Control	100.0	100.0	100.0	100.0	100.0
	Weeks Mean	95.6	90.8	70.0	56.9	78.3
	LSD 1 %		Weeks		WxT	
			0.62		1.52	
Disease severity %	**Chitosan NPs**	83.6	79.0	33.5	28.2	56.1
	Copper NPs	82.3	76.7	31.4	21.7	53.0
	Silver NPs	84.8	79.1	49.8	42.3	64.0
	Potassium Silicate	86.3	80.9	51.4	44.8	65.8
	Redomil gold	78.7	75.7	39.7	27.7	55.4
	Control	92.0	93.0	95.0	96.3	94.1
	Weeks Mean	84.6	80.7	50.1	43.5	64.7
	LSD 1 %		Weeks		WxT	
			0.84		2.05	

3.5. Plant Growth Parameters

All treatments, applied curatively, had a significant effect on basil plant growth parameters, including plant height, leaf number, leaf size, and fresh weight, as detailed in Table 4. The most

significant plant growth promotion was observed with Copper NPs (400 mg L^{-1}). This treatment produced the tallest plants (61.8 cm) and the highest number of leaves (71.8), significantly outperforming both the healthy Control (50.8 cm; 32.9 leaves) and the Redomil Gold fungicide (59.8 cm; 44.9 leaves). Chitosan NPs (400 mg L^{-1}) also showed outstanding results, producing the largest leaves (Length: 7.18 cm; Width: 4.98 cm), which were superior to both the Control and Redomil Gold. For plant fresh weight, both Copper NPs (400 mg L^{-1}) and Redomil Gold yielded the highest biomass (49.8 g), which was double the weight of the healthy Control (24.9 g). Chitosan NPs (400 mg L^{-1}) (48.8 g) and Potassium Silicate (3 g L^{-1}) (46.8 g) also produced excellent plant biomass. Conversely, Silver NPs at 50 mg L^{-1} showed the least positive effect, resulting in the lowest values for all growth parameters (e.g., 39.9 cm height; 19.9 g weight), which were significantly lower than the healthy Control, suggesting a mild phytotoxic effect or poor disease control at this concentration.

Table 5: The effect of different treatments on plant measurements.

Treatment	Con.	Plant height (cm)	No. of plant leaves	leaf length (cm)	Leaf width (cm)	Plant fresh weight (g)
Chitosan NPs	**50 mg L-1**	47.8	29.9	5.48	3.19	24.9
	100 mg L-1	49.8	33.9	5.58	3.29	29.9
	200 mg L-1	53.8	41.9	6.98	4.49	44.9
	400 mg L-1	55.8	64.8	7.18	4.98	48.8
Copper NPs	**50 mg L-1**	52.8	34.9	4.88	3.49	21.9
	100 mg L-1	54.8	63.8	5.98	3.49	29.9
	200 mg L-1	58.8	66.8	6.78	3.99	37.9
	400 mg L-1	61.8	71.8	7.08	4.98	49.8
Silver NPs	**50 mg L-1**	39.9	24.9	4.78	3.49	19.9
	100 mg L-1	41.9	27.9	5.58	3.69	20.9
	200 mg L-1	45.8	32.9	5.98	3.99	24.9
	400 mg L-1	48.8	34.9	6.48	4.19	29.9
Potassium silicate	**1 mL**	42.9	27.9	6.48	3.99	34.9
	1.5 mL	46.8	34.9	6.48	4.29	37.9
	2 mL	49.8	39.9	6.58	4.49	44.9
	3 mL	51.8	42.9	6.78	4.78	46.8
Redomil Gold MZ 68 WG		59.8	44.9	5.98	4.39	49.8
Control		50.8	32.9	5.68	3.69	24.9
LSD 1%	**Treatments**	0.3	0.7	0.03	0.03	0.56
	Cons.	0.2	0.5	0.03	0.02	0.46
	TxC	0.6	1.3	0.06	0.05	1.12

3.6. Leaf Anatomy (Histological Analysis)

Microscopical measurements of transverse leaf sections revealed significant histological changes induced by both the pathogen and the treatments (Table 5, Fig. 12). Compared to Healthy control, the Infected plants showed significant degradation and reduction in all measured parameters. This included a thinner upper epidermis (2.91 µm vs 3.54 µm in healthy), thinner palisade tissue (14.09 µm vs 17.22 µm), and a smaller vascular bundle (39.27 µm vs 48.80 µm). All treatments worked to mitigate this damage. Notably, Chitosan NPs (400 mg L^{-1}) and Potassium Silicate (3 g L^{-1}) provided the most significant protective and restorative effects. These treatments not only repaired the damage but *enhanced* the leaf structure to be stronger than the healthy control. Chitosan NPs produced the thickest tissues overall: upper epidermis (6.10 µm), lower epidermis (4.72 µm), spongy tissue (51.32 µm), palisade tissue (25.59 µm), and the largest vascular bundle (71.04 µm). Potassium Silicate was the second-best treatment, demonstrating a similar trend of anatomical enhancement. Copper NPs and Redomil Gold also restored tissue thickness to levels at or above the healthy control. Silver NPs was the least effective treatment, showing anatomical measurements (e.g., 3.04 µm upper epidermis) that were only slightly better than the infected plants and worse than the healthy control.

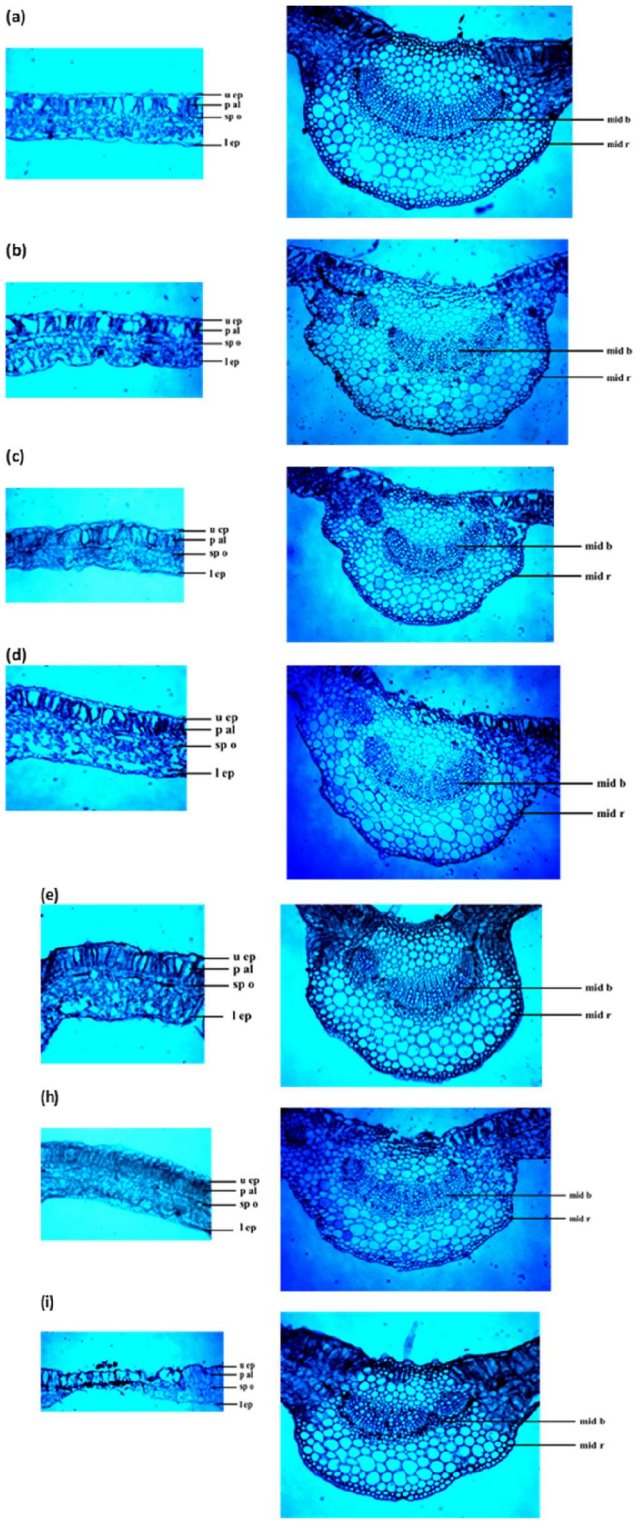

Fig. 13: Transverse sections through the lamina of the leaf developed at the median portion of the main stem of Basil plant, aged 45 days, (a) Chitosan, (b) potassium silicate, (c) Copper, (d) Ridomil gold, (e) Silver, (h) healthy and (i) infected.

Table 7: Measurements in micro-meter (µm) of certain histological features in transverse sections through the leaves of the basil plant, aged 12 weeks, treated by different compounds in comparison with the healthy plants and the infected plants.

Measurements	Chitosan NPs	Potassium silicate	Copper NPs	Silver NPs	Ridomil Gold	Healthy	Infected
Upper epidermis thickness	6.1	5.94	5.52	3.04	4.30	3.54	2.91
Lower epidermis thickness	4.72	4.44	3.94	2.53	3.41	2.84	2.33
Spongy tissue thickness	51.32	45.54	43.71	40.40	41.80	40.515	36.487
Palisade tissue thickness	25.59	24.80	19.51	16.23	18.43	17.220	14.085
Length of midrib vascular bundle	71.04	68.12	63.11	46.58	55.53	48.801	39.274
Thickness of leaf midrib	255.35	251.15	244.22	203.04	227.54	209.524	201.512

*Abbreviation: u. ep = upper epidermis, l. ep = lower epidermis, sp. o = spongy tissue thickness, p. al = palisade tissue thickness, mid b = length of midrib vascular bundle, and mid r = thickness of leaf midrib.

3.7. Biochemical Profile (Primary Metabolites)

The curative application of nanomaterials and other treatments significantly altered the primary biochemical composition of the basil plants (Table 8).

The most substantial improvements were seen in plants treated with Copper NPs (400 mg L^{-1}), which recorded the highest content of both total carbohydrates (3.09%) and total protein (16.54%). These values were significantly higher than those of the healthy Control (2.45% and 7.18%, respectively) and the Redomil Gold treatment (2.69% and 11.47%, respectively). This suggests a powerful restorative and growth-promoting effect. Chitosan NPs (400 mg L^{-1}) also showed excellent results, producing high levels of carbohydrates (2.79%) and protein (16.00%). Conversely, Silver NPs (50 mg L^{-1}) produced the lowest levels of carbohydrates (0.90%) and protein (7.17%), values that were significantly lower than the healthy Control, correlating with the poor plant growth observed in Table 4. For total lipids, CuNPs (400 mg L^{-1}) also recorded the highest content (0.708%), while Potassium Silicate (1 g L^{-1}) recorded the lowest (0.150%).

3.8. Plant Defense System Induction (Secondary Metabolites)

The analysis of plant defense compounds revealed a significant induction of systemic resistance by the nanoparticle treatments (Table 9).

Copper NPs (400 mg L^{-1}) triggered the strongest defense response, showing the highest accumulation of Total Phenols (11.56 mg/g) and the highest activities of all three defense-related enzymes: Catalase (1.51), Peroxidase (2.77), and Polyphenol Oxidase (0.97). Chitosan NPs (400 mg L^{-1}) also acted as a powerful elicitor, inducing the second-highest levels of Total Phenols (10.38 mg/g) and all associated enzymes. Critically, both CuNPs and CNPs at their highest concentrations induced a defense response that was significantly stronger than that of the Redomil Gold fungicide and the Healthy Control. This indicates that these nanoparticles provide a dual-action benefit: direct antifungal activity (as seen in Table 1) and a strong induction of the plant's own immune system. Potassium silicate and Silver NPs showed a weaker, though still dose-dependent, inductive effect.

Table 8: The effect of different treatments on plant total carbohydrates, total protein, and total lipids.

Treatment	Con.	Total Carbohydrates %	Total protein %	Total lipids %
Chitosan NPs	50 mg L^{-1}	1.69	8.60	0.468
	100 mg L^{-1}	1.89	11.27	0.538
	200 mg L^{-1}	2.29	14.98	0.648
	400 mg L^{-1}	2.79	16.00	0.668
Copper NPs	50 mg L^{-1}	1.50	10.16	0.588
	100 mg L^{-1}	1.79	11.03	0.618
	200 mg L^{-1}	2.59	15.61	0.638
	400 mg L^{-1}	3.09	16.54	0.708
Silver NPs	50 mg L^{-1}	0.90	7.17	0.299
	100 mg L^{-1}	1.30	11.22	0.329
	200 mg L^{-1}	1.99	12.13	0.458
	400 mg L^{-1}	2.29	14.29	0.498
Potassium silicate	1 mL	0.60	11.16	0.150
	1.5 mL	1.59	12.07	0.299
	2 mL	2.29	13.84	0.528
	3 mL	2.79	14.50	0.568
Redomil Gold MZ 68 WG		2.69	11.47	0.518
Control		2.45	7.18	0.449
LSD 1 %	Treatments	0.3	0.15	0.006
	Concentrations	**0.3**	**0.12**	**0.005**
	TxC	**0.6**	**0.29**	**0.013**

Table 9: The effect of different treatments on plant total phenols and defense enzymes (catalase – peroxidase - polyphenol oxidase)

Treatment	Con.	Total phenol (mg/g)	Enzymatic activities			Mean
			Catalase	Peroxidase	Polyphenol oxidase	
Chitosan NPs	50 mg L-^{1}	2.70	0.07	0.728	0.269	0.94
	100 mg L^{-1}	3.00	0.15	0.937	0.289	1.09
	200 mg L^{-1}	6.46	0.76	1.206	0.369	2.20
	400 mg L^{-1}	10.38	1.12	2.462	0.738	3.68
Copper NPs	50 mg L-^{1}	3.28	0.92	0.827	0.249	1.32
	100 mg L^{-1}	5.33	0.93	0.917	0.399	1.89
	200 mg L^{-1}	8.67	0.97	1.425	0.528	2.90
	400 mg L^{-1}	11.56	1.51	2.771	0.977	4.20
Silver NPs	50 mg L-^{1}	1.61	0.13	0.618	0.219	0.64
	100 mg L^{-1}	3.38	0.34	0.877	0.229	1.21
	200 mg L^{-1}	6.62	0.41	1.047	0.369	2.11
	400 mg L^{-1}	8.21	0.93	1.734	0.439	2.83
Potassium silicate	1 mL	1.39	0.08	0.389	0.239	0.52
	1.5 mL	2.60	0.14	0.817	0.259	0.95
	2 mL	4.63	0.59	1.096	0.488	1.70
	3 mL	6.58	0.77	1.355	0.488	2.30
Redomil Gold MZ 68 WG		6.39	0.83	1.186	0.608	2.25
Control		3.28	0.03	0.508	0.409	1.06
Mean		5.34	0.59	1.16	0.42	-
LSD 1 %	Treatments	0.13	0.02	0.029	0.009	-
	Concentrations	0.11	0.02	0.024	0.007	-
	TxC	0.27	0.04	0.058	0.018	-

3.9. Essential Oil Composition (GC Analysis)

Gas chromatography (GC) analysis of the essential oils extracted from the treated plants identified 18 primary chemical constituents. The results (Table 10) show that all treatments altered the chemical profile of the oil compared to the healthy control.

- **Chitosan NPs** application resulted in the highest concentrations of **Eugenol (10.69%)**, **1,8-Cineole (9.52%)**, α-Pinene (2.57%), Camphor (4.85%), and Chavicol (4.02%) compared to all other treatments.
- **Copper NPs** treatment led to the highest accumulation of **Linalool (19.58%)**, β-Pinene (2.19%), and Cadinol (4.31%).
- **Potassium Silicate** treatment resulted in the highest percentages of Sabinene (2.92%) and Limonene (3.61%).
- The **Redomil Gold** treatment, interestingly, produced the highest relative percentages of **Methyl Cinnamate (31.65%)** and Myrcene (2.94%).

The Healthy Control plants were characterized by having the highest levels of Methyl Chavicol (12.61%) and β-Caryophyllene (3.28%), compounds which were reduced in most of the nano-treated groups.

Table 10: Effect of the different treatments on the chemical composition of basil plant essential oil.

Component	Percentage %					
	Chitosan NPs	Copper NPs	Silver NPs	Potassium Silicate	Redomil gold	Control
α-pinene	2.57	1.94	1.32	1.38	1.59	1.75
sabinene	2.84	2.21	1.30	2.92	1.13	1.47
β-pinene	1.23	2.19	1.55	1.29	2.17	1.33
Myrcene	1.13	2.43	1.94	1.42	2.94	1.16
Limonene	3.12	2.11	1.15	3.61	2.26	2.94
1,8-cineol	9.52	7.83	5.97	6.71	8.14	8.48
α-terpinene	3.21	2.94	1.79	2.46	2.44	2.14
Linalool oxide	4.78	2.24	2.77	3.89	2.98	3.67
Linalool	18.76	19.58	11.97	16.54	12.63	14.85
Camphor	4.85	3.31	2.37	2.52	2.90	3.26
Methyl chavicol	9.01	9.36	7.30	10.87	8.27	12.61
Isoestragole	3.79	4.61	3.21	4.73	5.66	4.13
Chavicol	4.02	3.59	3.40	3.52	3.83	2.96
Bornyl acetate	3.55	2.91	2.60	3.53	3.31	2.33
Eugenol	10.69	7.35	8.13	7.04	5.76	9.34
Methyl cinnamate	27.39	29.92	24.16	25.41	31.65	25.24
β-caryophyllene	2.67	3.15	1.71	2.54	2.36	3.28
Cadinol	3.44	4.31	3.24	3.31	3.24	3.43
Sum	116.57	111.98	85.88	103.69	103.26	104.37

4. Discussion

The primary objective of this study was to evaluate eco-friendly nanomaterials for the management of basil downy mildew. The most significant finding was the successful curative application of biosynthesized nanoparticles. Notably, Copper Nanoparticles (CuNPs) at 400 mg L^{-1} not only controlled the disease but significantly outperformed the synthetic fungicide Redomil Gold (Table 3). This superior efficacy suggests that the nanoparticles employ a multi-pronged mechanism of action, encompassing both direct antifungal toxicity and the induction of host plant defenses.

Dual-Action Mechanism: Antifungal and Host-Defense Induction*:* The *in vitro* results (Table 1) confirmed the direct antifungal toxicity of all tested nanomaterials. The high inhibition rates are consistent with the established modes of action. For Chitosan (CNPs), its polycationic nature electrostatically interacts with the negatively charged fungal membrane, leading to altered cell permeability and leakage of cellular contents (García-Rincón *et al*., 2010). Furthermore, chitosan's chelating ability can sequester essential metal ions, making them unavailable for fungal development (Goy *et al*., 2009; Roller and Covill, 1999). Similarly, CuNPs are known for their broad-spectrum antimicrobial activity, which involves direct binding to the cell wall, membrane perforation, protein denaturation, and the induction of reactive oxygen species (ROS) that damage lipids and DNA (Mallick *et al*., 2012; Gaetke and Chow, 2003).

However, direct toxicity alone does not explain the superior *in vivo* curative success. The data strongly indicates that the nanoparticles also acted as powerful elicitors of the plant's own immune system. As shown in Table 9, CuNPs and CNPs triggered a significant accumulation of total phenols and defense-related enzymes (Peroxidase, Polyphenol Oxidase, and Catalase) far exceeding the levels in both healthy control and fungicide-treated plants. This is a hallmark of Systemic Acquired Resistance (SAR). These enzymes play a critical role in defense: PO and PPO catalyze the lignification and cross-linking of plant cell walls, creating a stronger physical barrier, while phenols act as direct antimicrobial compounds. This aligns perfectly with the findings of Siddaiah *et al*. (2018), who linked chitosan's control of pearl millet downy mildew directly to the stimulation of this innate immune pathway.

Nanoparticles such as Biostimulants: Enhancing Plant Anatomy and Physiology, beyond disease control, the treatments improved the plant's physical resilience and overall health. Anatomical analysis (Table 5) showed that CNPs and Potassium Silicate significantly increased the thickness of the leaf epidermis, palisade, and spongy tissues. This structural reinforcement creates a formidable physical barrier against initial pathogen penetration, which helps explain their strong performance in the preventive trial (Table 2). This finding is supported by Sharif *et al.* (2018) and El Amerany *et al*. (2020), who also reported anatomical improvements in plants treated with chitosan.

This biostimulant effect was further confirmed by the primary metabolite analysis (Table 8). Plants treated with CuNPs and CNPs showed the highest levels of total protein and total carbohydrates. This is a critical finding: the nanoparticles are not just stopping the pathogen; they are actively promoting plant health and photosynthesis. This enhanced metabolic state provides the plant with more energy and resources for both growth and defense, which directly explains the superior plant fresh weight (Table 4) and overall vigor. This agrees with Mau *et al*. (1999) and Michael and David (2002) regarding the role of proteins and carbohydrates in plant repair, growth, and energy.

Impact on Secondary Metabolism: Essential Oil Profile: The treatments also induced deep-seated changes in the plant's secondary metabolism, as evidenced by the essential oil profiles (Table 10). Each treatment modulated the oil's chemical composition differently, indicating specific interactions with plant metabolic pathways. For example, Chitosan NPs significantly boosted the concentration of the known antimicrobial compound Eugenol (10.69%), while Copper NPs led to the highest accumulation of Linalool (19.58%). This demonstrates that beyond disease control, the choice of nano-elicitor can be used to modulate the plant's final chemical profile and, potentially, its aromatic and medicinal quality. The data confirms that the nanomaterials had no negative effect on the diversity of the oil components.

5. Conclusion

In conclusion, this study demonstrates that biosynthesized Copper and Chitosan nanoparticles are highly effective and viable alternatives to synthetic fungicides for the management of basil downy mildew.

Most notably, Copper NPs (400 mg L^{-1}) exhibited a curative efficacy superior to the commercial fungicide Redomil Gold. This success is attributed to a dual-action mechanism: (1) direct antifungal toxicity and (2) a powerful induction of the plant's systemic resistance, evidenced by the accumulation of phenols and defense enzymes.

Furthermore, CuNPs and CNPs act as biostimulants, enhancing plant anatomical structure, promoting growth, and increasing the content of proteins and carbohydrates. These findings present a strong case for the use of CuNPs and CNPs as eco-friendly, multi-functional agents in an integrated pest management strategy, offering both disease control and plant health promotion.

References

Abd-Elsalam, K. A., & M. A. Alghuthaymi, 2015. Nanobiofungicides: are they the next-generation of fungicides. *J Nanotech Mater Sci*, *2*(2), 38-40.

Abu-Elsaoud, A. M., A. M. Abdel-Azeem, S. A. Mousa and S. S. Hassan, 2015. Biosynthesis, optimisation and photostimulation of [alpha]-NADPH-dependent nitrate reductase-mediated silver nanoparticles by Egyptian endophytic fungi. Advances in Environmental Biology, 9(24): 259-270.

Abdullah E., M., R.N. Fawzy, K.S. Eid, A.M. Gowily, , M.K.M. Agha and G.A. Ahmed, 2022. Pathological and physiological studies of Downy Mildew of Basil (*Ocimum basilicum*) Caused by *Peronospora belbahrii* in Egypt. Benha Journal of Applied Sciences, *7*(4): 25-37.

Alghuthaymi, M. A., H. Almoammar, M. Rai, E. Said-Galiev & K. A. Abd-Elsalam, 2015. Myconanoparticles: synthesis and their role in phytopathogens management. Biotechnology & Biotechnological Equipment, 29(2): 221-236.

Allam, A.I., and J.P. Hollis, 1972. Sulfide inhibition of oxidases in rice roots. Phytopathology, 62,634-639.

Bhattacharya, D., & R. K Gupta, 2005. Nanotechnology and potential of microorganisms. Crit Rev Biotech, 25(4):199-204.

British Pharmacopoeia, 1993. Published on the pharmaceutical press. London; W.C.I.; 2:146A.

Chaplin M.F. and J.F. Kennedy, 1994. In "Carbohydrates Analysis. A Practical Approach". Oxford University Press, Oxford, New York., Tokyo. 2nd Ed, pp: 324.

Christie, W.W., 1982. Lipid Analysis. Pergamon Press, 2nd Ed.: 207 pp.

Duncan, D.B., 1955. Multiple ranges and multiple F. test. Biometrics, (11):11-24.

El Amerany, F., M. Rhazi, S. Wahbi, M. Taourirte and A. Meddich, 2020. The effect of chitosan, arbuscular mycorrhizal fungi, and compost applied individually or in combination on growth, nutrient uptake, and stem anatomy of tomato. Scientia Horticulturae, 261, 109015.

Gaetke, L. M., and C. K. Chow, 2003. Copper toxicity, oxidative stress, and antioxidant nutrients. Toxicology, 189(1-2), 147-163.

García-Rincón, J., J. Vega-Pérez, M. G. Guerra-Sanchez, A. N. Hernandez-Lauzardo, A. Peña-Díaz and M. G. Velazquez-Del Valle, 2010. Effect of chitosan on growth and plasma membrane properties of *Rhizopus stolonifer* (Ehrenb.: Fr.) Vuill. Pesticide Biochemistry and Physiology, 97(3), 275-278.

Ghebrial, E., and A.A.A. Dewidar, 2020. Determining the susceptibility of different basil varieties to downy mildew caused by *Peronospora belbahrii.* Journal of Plant Pathology and Microbiology. 11(7), 502-512.

Ghebrial, E.W.R. and M.G.A. Nada, 2017. Suppression of basil downy mildew caused by *Peronospora belbahrii* using resistance inducers, mineral salts and antitranspirants combined with different rates of nitrogen fertilizer under field conditions. Egyptian Journal of Phytopathology, 45(1), 71-97.

Gomez, K.A. and A.A. Gomez, 1984. Statistical procedures for agricultural Res. 2nd ed. Wiley, New York.

Goth, L., 1991. A simple method for determination of serum catalase activity and revision of reference range. *Clinica chimica acta*, 196(2-3), 143-151.

Goy, R. C., D. D. Britto and O. B. Assis, 2009. A review of the antimicrobial activity of chitosan. Polímeros, 19(3): 241-247.

Guenther, E., 1961. The Essential Oils. Vol. IV, Nostrand Co. Inc., New York.

Kasprowicz, M. J., M. Kozioł and A. Gorczyca, 2010. The effect of silver nanoparticles on phytopathogenic spores of *Fusarium culmorum.* Canadian Journal of Microbiology, 56(3):247-253.

Kaur, C., and H. C. Kapoor, 2002. Antioxidant activity and total phenolic content of some Asian vegetables. International Journal of Food Science and Technology, 37(2), 153-161.

Kim, S. W., K. S. Kim, K. Lamsal, Y. J. Kim, S. B. Kim, J. M. Y.ung,.. & Y. S. Lee, 2009. An in vitro study of the antifungal effect of silver nanoparticles on oak wilt pathogen Raffaelea sp. Journal of Microbiology and Biotechnology, 19(8), 760-764.

Koul, A., C. Becchio and A. Cavallo, 2018. Cross-validation approaches for replicability in psychology. Frontiers in Psychology, 9, 1117.

Krolikowska, A., A. Kudelski, A. Michota & J. Bukowska, 2003. SERS studies on the structure of thioglycolic acid monolaye rs on silver and gold. Surface science, 532, 227-232.

Li, G., D. He, Y. Qian, B. Guan, S. Gao, Y. Cui, ... & L. Wang, 2011. Fungus-mediated green synthesis of silver nanoparticles using Aspergillus terreus. International Journal of Molecular Sciences, 13(1), 466-476.

Mallick, S., S. Sharma, M. Banerjee, S. S. Ghosh, A. Chattopadhyay and A. Paul, 2012. Iodine-stabilized Cu nanoparticle chitosan composite for antibacterial applications. ACS applied materials and Interfaces, 4(3), 1313-1323.

Matta, A., and A.E. Diamond, 1963. Symptoms of *fusarium* wilt in relation to quantity of *fusarium* and enzyme activity in tomato stem. Phytopathology. 53(5), 574-578.

Mau, J. L., M.B. Miklus and R.B. Beelman, 1999. Shelf-life studies of foods and *Beverages charalambous* E.d. Chemistry of Biological Physics Nutritional Aspects, 57: 475-477.

Michael, K. and M. David, 2002. The useful plants of West Tropical Africa. Nigerian Journal of Biochemical Molecular Biology, 12: 53-60.

Nassar, M.A., and K. F. El-Sahhar, 1998. Botanical preparations and microscopy (Microtechnique). Academic Bookshop, Dokki, Giza, Egypt, 219.

Okey-Onyesolu, C. F., E. U. Dike & E. N. Onyeneke, 2021. A review on the antifungal properties of copper, silver and chitosan nanoparticles on plant-pathogenic fungi. Journal of Plant Diseases and Protection, 128(4), 867–883.

Roller, S., and N. Covill, 1999. The antifungal properties of chitosan in laboratory media and apple juice. International journal of food microbiology, 47(1-2), 67-77.

Shantkriti, S. and P. Rani, 2014. Biological synthesis of copper nanoparticles using Pseudomonas fluorescens. International Journal of Current Microbiology and Applied Sciences, 3(9), 374-383.

Sharif, R., M. Mujtaba, M. Ur Rahman, A. Shalmani, H. Ahmad, T. Anwar and X. Wang, 2018. The multifunctional role of chitosan in horticultural crops; a review. Molecules, 23(4), 872.

Siddaiah, C. N., K. V. H. Prasanth, N. R. Satyanarayana, V. Mudili, V. K. Gupta, N. K. Kalagatur, and R. K. Srivastava, 2018. Chitosan nanoparticles having higher degree of acetylation induce resistance against pearl millet downy mildew through nitric oxide generation. Scientific reports, 8(1), 1-14.

Simon, J. E., M. R. Morales, P. W. B.hippen, V. R. F.ieira, and Z. Hao, 1999. Basil: a source of aroma compounds and a popular culinary and ornamental herb. Perspectives on new crops and new uses, 16, 499-505.

Tang, Z. X., J. Q. Qian, and L. E. Shi, 2007. Preparation of chitosan nanoparticles as carrier for immobilized enzyme. Applied Biochemistry and Biotechnology, 136(1):77-96.

Wyenandt, C.A., J.E. Simon, R.M. Pyne, K. Homa, M.T. McGrath, S. Zhang, R.N. Raid, L.J. Ma, R. Wick, and L. Guo and A. Madeiras, 2015. Basil downy mildew (Peronospora belbahrii): discoveries and challenges relative to its control. Phytopathology 105, 885e894.